JOURNAL OF MATERIALS SCIENCE 28 (1993) 5957–5962

Hardness and mechanical property relationships in directionally solidified aluminium–silicon eutectic alloys with different silicon morphologies

S. KHAN
Research Laboratories, G.P.O. Box 502, Rawalpindi, Pakistan
A. OURDJINI, Q. S. HAMED, M. A. ALAM NAJAFABADI, and R. ELLIOTT
Manchester Materials Science Centre, University of Manchester, Grosvenor Street, Manchester M1 7HS, UK

Hardness and tensile property measurements made on directionally solidified Al–Si eutectic alloys show that definite but different hardness–growth velocity and hardness–silicon interparticle spacing relationships exist for alloys with different silicon eutectic phase morphologies. Tensile property measurements show that hardness and 0.2% proof stress follow silicon interparticle spacing relationships of the same form. It is suggested that hardness can only be used to measure proof stress when the eutectic structure displays a single silicon eutectic phase morphology.

1. Introduction

Structural refinement improves the strength and ductility of a material. In the case of grain refinement the effect of grain size can be expressed by the relationship

$$\sigma_{YS} = \sigma_0 + K_1 d^{-0.5} \quad (1)$$

where d is the grain diameter, σ_0 is the flow stress of the matrix and K_1 is a constant. This is known as the Hall–Petch relationship [1] and is based on a model that considers grain boundaries as obstacles to dislocation motion.

Directionally solidified eutectic alloys or *in situ* composites have been used to improve the strength, stability, creep and corrosion resistance of single-phase alloys at room and elevated temperatures [2]. It is well established that reducing the eutectic particle spacing improves the mechanical properties and that hardness mirrors mechanical property behaviour. Several studies have expressed the influence of structural refinement in terms of Equation 1, although there is doubt as to whether dislocation pile-ups occur during the deformation of *in situ* composites.

The Al–Si eutectic is the basis of several important casting alloys. It falls into the category of a ductile/brittle *in situ* composite but its behaviour is complicated by the fact that as growth velocity increases and temperature gradient in the liquid decreases, the eutectic silicon morphology changes from rod-like angular silicon to flaky silicon to fibrous silicon and a complex regular morphology forms in areas enriched in silicon. It has been shown [3–5] that hardness and yield stress obey a Hall–Petch relationship when silicon solidifies in the rod-like angular silicon morphology. Telli and Kisakurek [6, 7] have presented hardness measurements, tensile properties and structural features of directionally solidified Al–Si eutectic alloys displaying the flaky silicon morphology in the untreated condition and refined with antimony. They showed that hardness and tensile properties showed similar dependencies on growth velocity and silicon interflake spacing. In particular, they concluded that the relationships between interflake spacing, growth velocity, temperature gradient and concentration of antimony are such that a single relationship exists between mechanical properties and interflake spacing and this is of the Hall–Petch type. The existence of such a relationship and the corresponding one between hardness and spacing, provide a useful means of assessing the mechanical properties of Al–Si or antimony-refined Al–Si flake eutectic alloys without a knowledge of the solidification conditions. Recently [8], we have questioned the existence of a Hall–Petch relationship for the flake eutectic structure. Also, it has been shown [5] that in the presence of the complex regular silicon morphology, considerable deviations occur in the hardness–spacing relationship. These findings throw doubt on the suggestions made by Telli and Kisakurek.

The purpose of the present paper is to report measurements made on untreated, antimony-refined and strontium-modified directionally solidified Al–Si eutectic alloys using a wider range of growth velocities than used previously, to test Telli and Kisakurek's

0022–2461

suggestion further, and define the hardness–spacing relationship for alloys showing the fibrous silicon morphology produced by chilling and strontium modification.

2. Experimental procedure

Alloys of composition Al–12.7 wt % Si and Al–14.6 wt % Si were prepared using metals of 99.999% purity. Weighed amounts of aluminium and silicon were melted under argon and after melt homogenization for 15 min were sucked into alumina tubes 200 mm in length and 7 mm outer diameter. The remaining melt was quenched and used for analysis. The alloys were remelted in a vertical Bridgman directional solidification apparatus and, after allowing 20 min for melt stabilization, were solidified by withdrawing the specimen into a water-cooled water reservoir at a constant traction velocity in the range 0.10–1080 $\mu m\,s^{-1}$. It has been shown [9] that with a Bridgman-type furnace there exists a critical growth velocity above which the interface growth velocity falls below the traction velocity. Consequently, fine thermocouples embedded in the specimen were used to record cooling curves from which the growth velocity and temperature gradient in the melt were measured. The growth velocity was found to deviate from the traction velocity above 108 $\mu m\,s^{-1}$ and the temperature gradient was found to change slightly (maximum 4%) as the growth velocity increased. A few measurements were made on alloys solidified with a low temperature gradient. These alloys were cast, after melting as described above, into graphite boats 190 mm × 13 mm × 10 mm. These specimens were solidified under argon in a thermal valve furnace. This directional solidification apparatus has been described in detail elsewhere [10]. Some melts were treated with strontium in the form of an Al–10% Sr master alloy, or antimony metal prior to casting into the alumina tubes. Longitudinal and transverse sections were cut from the specimens after 60 mm of growth and prepared for optical microscopy. A linear intercept method was used to measure the interrod and interflake eutectic spacings. Interfibre spacing was measured from a photograph of a transverse section of magnification, M, by counting the number of fibres, N, within a known area, A. The average interfibre spacing was calculated from the equation

$$\lambda = \frac{1}{M}\left(\frac{A}{N}\right)^{0.5} \quad (2)$$

Finally, Vickers hardness measurements were made on the transverse sections using either a 1 or 2 kg load depending on the silicon spacing. Each hardness is the average of at least two measurements.

3. Results and discussion

Alloys containing 14.6 wt % Si were used at higher growth velocities in order to promote solidification within the coupled zone [11] and to avoid primary phase formation. The different silicon morphologies studied are shown in Fig. 1. Fig. 2 shows the variation of hardness with growth velocity for the angular silicon, flaky silicon and quench-modified fibrous silicon morphologies. The results confirm previous observations that the hardness increases as the growth velocity increases and shows clearly that different relationships exist for the different silicon morphologies. All the measurements can be represented by an equation of the form

$$H = H_0 + Kv^n \quad (3)$$

where H_0 is the initial hardness. The value of n for the angular silicon morphology is 0.22 which is close to the previously measured value of 0.25 [3, 5]. The value of n for the flaky silicon morphology is 0.12. This is considerably less than the value for the angular silicon morphology and similar but slightly greater than previous measurements for alloys solidified at different temperature gradients [5, 8] ($n = 0.04$) and measurements made by Telli and Kisakurek [7] ($n = 0.08$). The value of n for the quenched modified fibrous silicon morphology in 0.04, which is in good agreement with previous measurements [5]. Similar relationships were found for the different silicon morphologies in alloys containing 0.2% Sb. However, the hardness was greater in alloys treated with antimony. The increased value of H_0 for antimony-treated alloys can be attributed to silicon particle spacing refinement and aluminium solid-solution hardening. The slight increase in hardness with increasing temperature gradient for the flaky structure can be attributed to particle refinement. Fig. 3 shows the hardness–growth velocity relationship for the silicon fibrous morphology produced by quench modification in Al–Si and Al–Si–Sb alloys and strontium modification in Al–Si alloys and solidified with different temperature gradients in the melt. All these measurements can be described by Equation 3 with a value of $n = 0.04$.

The hardness of the strontium-modified fibrous morphology shows a slight dependence on temperature gradient in the melt during solidification. This dependence is not as clearly defined for quench-modified fibres.

The variation of interparticle spacing with growth velocity is shown in Fig. 4 for the angular silicon morphology and the flaky silicon morphology. The results can be fitted to a relationship of the form

$$\lambda = Kv^{-m}\ (\mu m\,s) \quad (4)$$

The values of K and m are 10 and 0.5, respectively for the angular silicon morphology. Additions of antimony refine the structure to give values of K and m of 7.1 and 0.5, respectively. There have been several previous studies of the variation of interflake spacing with growth velocity [8, 12–14]. All the measurements have been expressed in terms of Equation 4 with m varying between 0.33 and 0.50. These studies have also established that the interflake spacing is temperature gradient dependent; the spacing decreases as the temperature gradient increases. The present measurements for flaky silicon for a temperature gradient of 122 °C cm^{-1} obey Equation 4 with K and m values of 0.48 and 0.42, respectively. A slightly higher K value describes the measurements at a temperature gradient

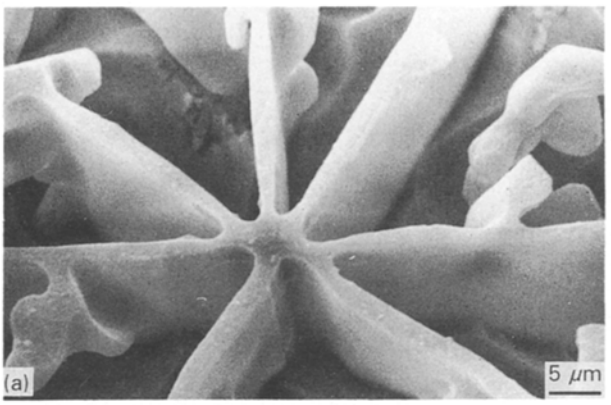

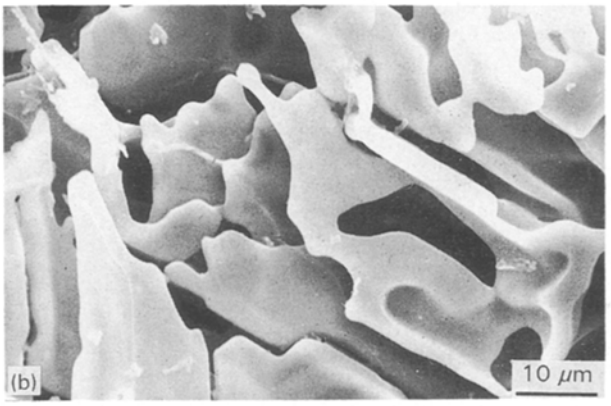

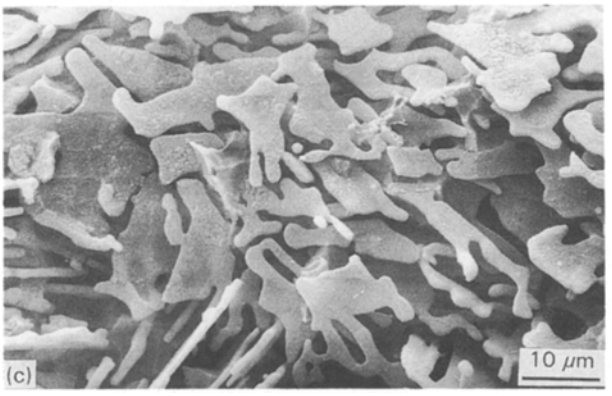

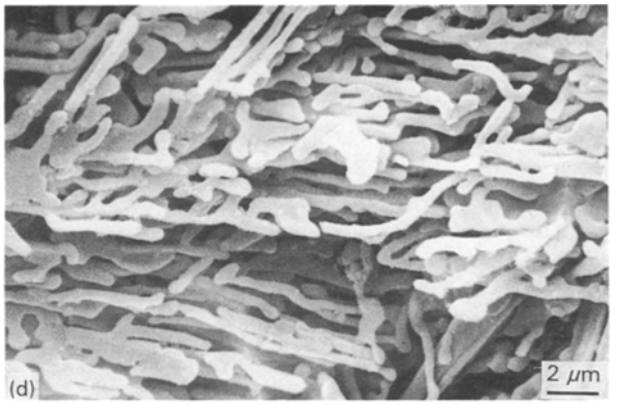

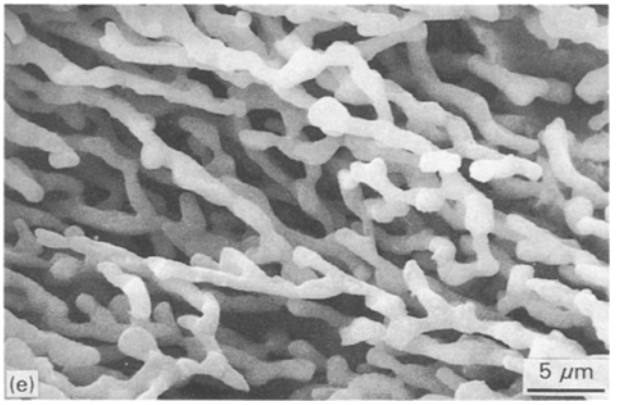

Figure 1 Scanning electron micrographs of the eutectic silicon morphologies. (a) Al–Si, $G = 129\,^{\circ}C\,cm^{-1}$, $v = 1.35\,\mu m\,s^{-1}$, angular silicon. (b) Al–Si, $G = 32\,^{\circ}C\,cm^{-1}$, $v = 81\,\mu m\,s^{-1}$, flaky silicon. (c) Al–Si–Sb, $G = 32\,^{\circ}C\,cm^{-1}$, $v = 81\,\mu m\,s^{-1}$, flaky silicon. (d) Al–Si, $G = 129\,^{\circ}C\,cm^{-1}$, $v = 820\,\mu m\,s^{-1}$, quenched fibrous silicon. (e) Al–Si–Sr, $G = 82\,^{\circ}C\,cm^{-1}$, $v = 54\,\mu m\,s^{-1}$, strontium-modified fibrous silicon.

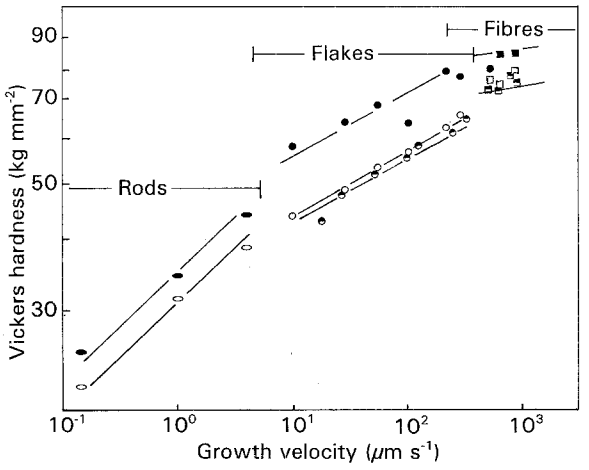

Figure 2 Variation of hardness with growth velocity. (○) Al–12.7% Si, $G = 122\,^{\circ}C\,cm^{-1}$, angular silicon; (◒) Al–12.7% Si–0.2% Sb, $G = 122\,^{\circ}C\,cm^{-1}$, angular silicon; (○) Al–12.7% Si, $G = 122\,^{\circ}C\,cm^{-1}$, flaky silicon; (◓) Al–12.7% Si, $G = 82\,^{\circ}C\,cm^{-1}$, flaky silicon; (●) Al–12.7% Si–0.2% Sb, $G = 122\,^{\circ}C\,cm^{-1}$ flaky silicon; (□) Al–14.6% Si, $G = 122\,^{\circ}C\,cm^{-1}$, quenched fibrous silicon; (◨) Al–14.6% Si, $G = 82\,^{\circ}C\,cm^{-1}$, quenched fibrous silicon; (■) Al–12.7% Si–0.2% Sb, $G = 122\,^{\circ}C\,cm^{-1}$, quenched fibrous silicon.

of $82\,^{\circ}C\,cm^{-1}$. The addition of antimony refines and does not modify the eutectic structure as described elsewhere [15]. The variation of interflake spacing with growth velocity for alloys treated with antimony can be described by Equation 4 with K and m values of 0.40. Fig. 4 also shows the interflake spacing measurements made by Telli and Kisakurek. They were fitted to Equation 4 with K and m values of 3.7 and 0.19, respectively, for Al–Si alloys and of 3.8 and 0.06 for alloys treated with antimony. The m values defining these results do not conform with values accepted as being typical of flaky silicon eutectic growth and, indeed they do not confirm that antimony refines the flake structure. Fig. 5 shows the variation of interfibre spacing with growth velocity for strontium and quench-modified alloys solidifed with different temperature gradients in the melt. The results for the fibrous silicon morphology produced by strontium treatment can be fitted to Equation 4 with $m = 0.54$ and K varying from 0.21–0.19 as the temperature gradient increases. The results for the quench-modified alloys can be fitted to Equation 4 with K and m values of 0.20 and 0.50, respectively. There is a variation in the K value which is difficult to relate to temperature gradient and antimony refinement with

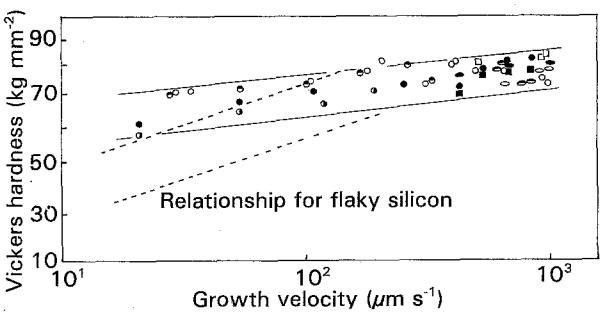

Figure 3 Variation of hardness with growth velocity. (○) Al–Si–Sr, $G = 122\,^{\circ}C\,cm^{-1}$, strontium-modified fibrous silicon; (◓) Al–Si–Sr, $G = 82\,^{\circ}C\,cm^{-1}$, strontium-modified fibrous silicon; (●) Al–Si–Sr, $G = 32\,^{\circ}C\,cm^{-1}$, strontium-modified fibrous silicon; (◑) Al–Si–Sr, $G = 5\,^{\circ}C\,cm^{-1}$, strontium-modified fibrous silicon; (⌓) Al–Si, $G = 122\,^{\circ}C\,cm^{-1}$, quenched fibrous silicon; (◓) Al–Si, $G = 82\,^{\circ}C\,cm^{-1}$, quenched fibrous silicon; (◒) Al–Si, $G = 32\,^{\circ}C\,cm^{-1}$, quenched fibrous silicon; (□) Al–Si–Sb, $G = 122\,^{\circ}C\,cm^{-1}$, quenched fibrous silicon; (■) Al–Si–Sb, $G = 32\,^{\circ}C\,cm^{-1}$, quenched fibrous silicon.

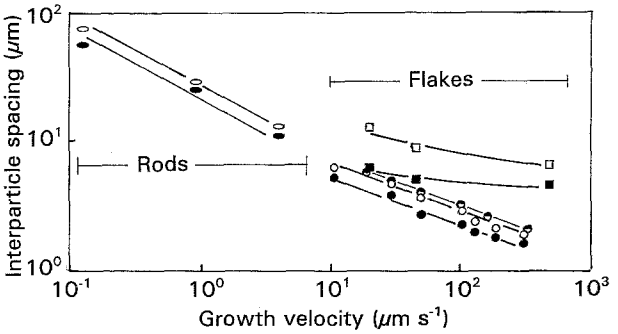

Figure 4 Variation of silicon interparticle spacing with growth velocity. (⌓) Al–Si, $G = 122\,^{\circ}C\,cm^{-1}$, angular silicon; (◒) Al–Si–Sb, $G = 122\,^{\circ}C\,cm^{-1}$, angular silicon; (○) Al–Si, $G = 122\,^{\circ}C\,cm^{-1}$, flaky silicon; (◓) Al–Si, $G = 82\,^{\circ}C\,cm^{-1}$, flaky silicon; (●) Al–Si–Sb, $G = 122\,^{\circ}C\,cm^{-1}$, flaky silicon; (□) Al–Si, Telli and Kisakurek [7], flaky silicon; (■) Al–Si–Sb, Telli and Kisakurek [7], flaky silicon.

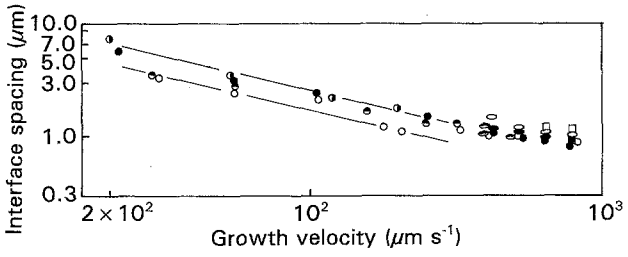

Figure 5 Variation of interfibre silicon spacing with growth velocity. For key, see Fig. 3.

the present results. However, the relationships for the fibrous silicon morphologies are similar and different from the relationships for the flaky silicon morphology indicating the different growth modes of the two structures.

The results given so far can be used to define the hardness–silicon interparticle spacing relationship for each eutectic silicon morphology. Fig. 6 shows the relationships for the angular silicon morphology, flake morphology and quench-modified fibre morphology. Fig. 7 shows the relationship for the fibrous morphology produced by quench modification and strontium modification. These figures show that the hardness decreases as the interparticle spacing increases and that there is a distinct relationship for each silicon morphology. Each can be fitted to an equation of the form

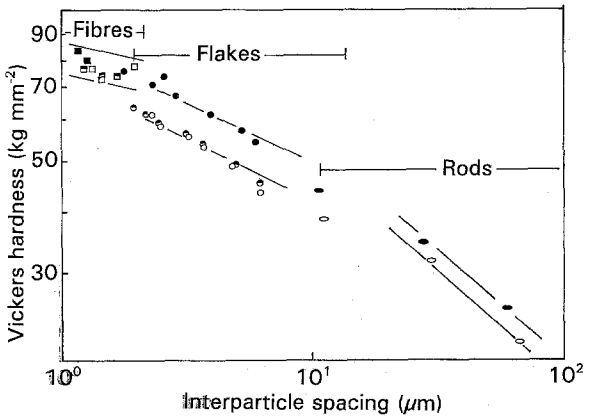

Figure 6 Variation of hardness with silicon interparticle spacing. For key, see Fig. 2.

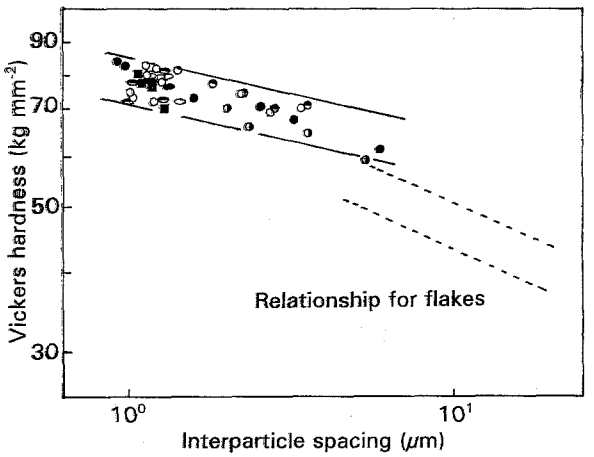

Figure 7 Variation of hardness with silicon interfibre spacing. For key, see Fig. 3.

$$H = H_0 + A\lambda^{-d} \quad (5)$$

with values of $d = 0.50$, 0.22 and 0.10 for the angular silicon morphology, flaky silicon morphology and the fibrous silicon morphology, respectively. The findings for the angular silicon morphology confirm those of Justi and Bragg [3, 4]. The measurements for this morphology in alloys treated with antimony can be described by Equation 5 with an increased value of H_0. This increase is probably due to aluminium solid-solution hardening by antimony. The results for the flake morphology do not confirm those of Telli and Kisakurek [7]. The value of $d = 0.22$ shows good agreement with the value of 0.20 measured for Al–Si eutectic alloys solidified with different temperature gradients in the melt [9] and does not confirm the value of 0.50 suggested by Telli and Kisakurek. Alloys treated with antimony obey the same relationship with a higher value of H_0. This is attributed to solid-solution hardening. The discrepancy between the present measurements and those of Telli and Kisakurek

[7] arise from the different spacing–growth velocity relationships recorded in the two studies. The present measurements do not confirm a Hall–Petch type of relationship for the flake morphology and nor do they confirm a universal relationship for the flake morphology. The value of $d = 0.10$ for the fibrous silicon morphology shows good agreement with previous measurements [5]. The measurements in Fig. 7 show some scatter about a mean relationship. This is not surprising when it is realized that the measurements were made on the fibrous morphology produced by quench and impurity modification in untreated, strontium- and antimony-treated alloys of two silicon contents and with different temperature gradients in the liquid during solidification.

Finally tensile tests were performed on Al–12.7 wt % Si alloys displaying the flaky silicon morphology and the fibrous silicon morphology produced by strontium treatment. Specimens were machined from specimens grown in the thermal valve furnace over a range of growth velocities with a temperature gradient of 10 °C cm^{-1} in the melt. The variation of ultimate tensile strength (UTS) and 0.2% proof stress with growth velocity is shown in Fig. 8. A slight increase in both properties is evident for the antimony-treated alloys for the same solidification conditions. This is in keeping with the fact that antimony only refines the flaky silicon. The increase in both properties due to strontium modification is evident at the lower growth velocities in particular. These conditions are the conditions encountered in sand casting when strontium treatment results in a significant increase in properties. The results are plotted as a function of silicon interparticle spacing in Fig. 9. This figure shows that for the flaky and fibrous silicon morphologies, the variation of UTS and 0.2% proof stress can be described by an equation of the form

$$\sigma = \sigma_0 + B\lambda^{-f} \quad (6)$$

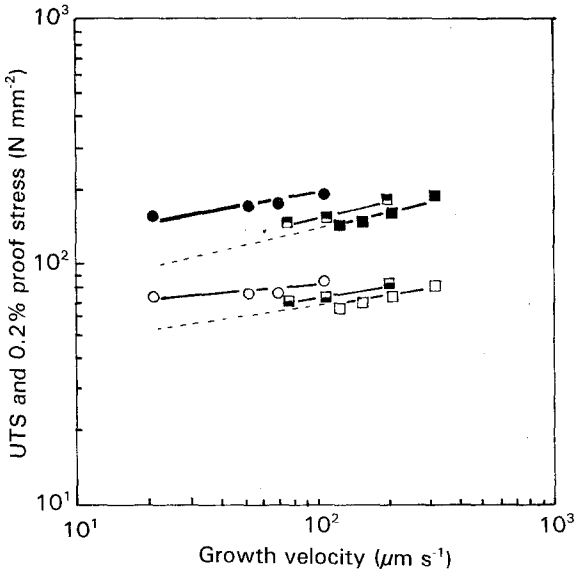

Figure 8 Variation of UTS and 0.2% proof stress with growth velocity. (■) Al–Si, flaky silicon, UTS; (□) Al–Si, flaky silicon, 0.2% proof stress; (▬) Al–Si–Sb, flaky silicon, UTS; (▭) Al–Si–Sb, flaky silicon, 0.2% proof stress; (●) Al–Si–Sr, fibrous silicon, UTS; (○) Al–Si–Sr, fibrous silicon, 0.2% proof stress.

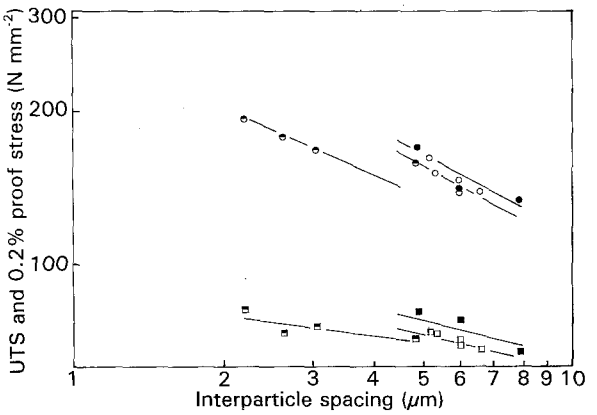

Figure 9 Variation of UTS and 0.2% proof stress with silicon interparticle spacing. (○) Al–Si, flaky silicon, UTS; (●) Al–Si–Sb, flaky silicon, UTS; (□) Al–Si, flaky silicon, 0.2% proof stress; (■) Al–Si–Sb, flaky silicon, 0.2% proof stress; (◓) Al–Si–Sr, fibrous silicon, UTS; (▬) Al–Si–Sr, fibrous silicon, 0.2% proof stress.

with values of $f = 0.50, 0.45, 0.20$ and 0.12 for the UTS of flaky silicon, the UTS of fibrous silicon, the 0.2% proof stress of flaky silicon and the 0.2% proof stress of fibrous silicon, respectively. This figure shows that the relationships for flaky silicon with and without antimony can be described by Equation 6 with different values of σ_0. It also shows that the hardness–spacing and the 0.2% proof stress–spacing relationships for flaky silicon and strontium-modified fibrous silicon are of a similar form.

4. Conclusions

Hardness measurements made on directionally solidified Al–Si eutectic alloys showing the angular, flaky or fibrous silicon eutectic morphology show that there are different hardness–interparticle spacing relationships for each silicon morphology. Tensile tests show that the hardness–spacing relationship is of the same form as the 0.2% proof stress–spacing relationship for the flaky and fibrous morphologies. These observations confirm previous conclusions that hardness measurements cannot be used to predict mechanical properties unless the structure displays a single eutectic silicon morphology.

Acknowledgements

The authors thank Professor F. R. Sale for providing laboratory facilities. Financial assistance from the Government of Pakistan (S. K.) and the British Council and Government of Algeria (A. O.) is acknowledged. R. E. acknowledges the continued support of Alcoa, Pittsburgh, USA for directional solidification studies of aluminium alloys.

References

1. N. J. PETCH, *J. Iron Steel Inst.* **173** (1953) 25.
2. R. ELLIOTT, "Eutectic Solidification Processing" (Butterworths, London, 1983).
3. S. JUSTI and R. H. BRAGG, *Metall. Trans.* **7A** (1976) 1954.
4. *Idem, ibid.* **9A** (1978) 515.

5. F. YILMAZ and R. ELLIOTT, *J. Mater. Sci.* **24** (1989) 2065.
6. S. E. KISAKUREK, in "Proceedings of the Conference 53rd World Foundry Congress", Prague, Czechoslovakia, September 1986.
7. A. I. TELLI and S. E. KISAKUREK, *Mater. Sci. Technol.* **4** (1988) 153.
8. A. OURDJINI, F. YILMAZ, Q. S. HAMID and R. ELLIOTT, *ibid.* **8** (1992) 774.
9. S. KHAN, A. OURDJINI and R. ELLIOTT, *ibid.* **8** (1992) 516.
10. Q. S. HAMID and R. ELLIOTT, *Cast Metals J.*, **6** (1993) 36.
11. F. YILMAZ, O. A. ATASOY and R. ELLIOTT, *J. Crystal Growth* **118** (1992) 377.
12. B. TOLOUI and A. HELLAWELL, *Acta Metall.* **24** (1976) 565.
13. R. ELLIOTT, in "Proceedings of the 2nd International Conference on Aluminium Melt Treatment" Paper 10, (A. F. S., Orlando, 1989).
14. S. KHAN and R. ELLIOTT, *Acta Metall.*, submitted (1993).
15. *Idem*, J. Mat. Sci. submitted (1993).

Received 16 February 1993
and accepted 19 March 1993